

Optical properties of potassium clusters incorporated into zeolite LTA

Tetsuya Kodaira, Yasuo Nozue, Satoshi Ohwashi, Takenari Goto, and Osamu Terasaki
Department of Physics, Faculty of Science, Tohoku University, Aramaki, Aoba-ku, Sendai 980, Japan
 (Received 25 March 1993)

Optical properties are reported for cationic K clusters incorporated into the α cage of K-form LTA. The α cage has an inside diameter of ~ 11 Å and is arrayed in a simple cubic structure. The loading density of potassium is systematically changed from dilute to saturated conditions. The average number of guest K atoms is 7.3 per α cage at the saturation density. Three groups of absorption and/or reflection bands appear depending on the K loading density. A band at ~ 2 eV increases and becomes the strongest reflection band with increasing K density, and is assigned to the surface-plasmon-like state of the K cluster. Other groups of bands are relatively weak and are interpreted in terms of the model of the transition between energy bands which originate from $1s$, $1p$, and $1d$ molecular orbitals of the K cluster. A Drude-like contribution is found in the analysis of reflection spectra. This is reminiscent of the metallic state of arrayed clusters.

I. INTRODUCTION

Recently, optical properties of small alkali-metal clusters have been investigated intensively using photodissociation spectroscopy of free clusters¹⁻¹² and spectroscopy of zeolite-supported clusters.^{13,14} In these clusters, photoexcitation due to the collective motion of the electrons, called a surface-plasmon (SP) state, and the individual electron excitation between molecular orbitals of the cluster have been observed. Theoretically, there has been much interest in the optical excitation of metal clusters.¹⁵⁻²⁸

The framework of zeolite crystals includes well-defined cages or channels specific to their type. New material designs have been expected to exist in the zeolite space.²⁹ In Na-form FAU (faujasite), which is usually called NaY, the Na_4^{3+} paramagnetic cluster has been observed in the color change and the ESR measurement.³⁰ Various kinds of alkali-metal clusters have been investigated in FAU (Refs. 31-38) and SOD (sodalite).³⁹⁻⁴¹

LTA, which is a type of zeolite, has the framework structure shown schematically in Fig. 1. In this figure, oxygen atoms between Si and Al atoms are omitted. An α cage (supercage) with an inside diameter of ~ 11 Å is surrounded by eight β cages (sodalite cages). Si and Al atoms are expected to be arranged alternately according to the Loewenstein rule.⁴² The α cages are arrayed in a simple cubic structure with the lattice constant of 12.3 Å and are connected by shared windows with an inner diameter of ~ 5 Å. In ideal Na form LTA, 12 Na^+ ions are distributed in the space of the framework. The chemical formula is given as $\text{Na}_{12}\text{Al}_{12}\text{Si}_{12}\text{O}_{48}$.

In a previous paper,¹³ absorption spectra have been reported for sodium clusters incorporated into Na-form LTA zeolite. Clusters in the α and β cages have been observed. Spectra of clusters in the α cage have exhibited an SP-like excitation as well as transitions between discrete energy levels of the cluster. In potassium clusters incorporated into K-form LTA, ferromagnetism has

been observed at low temperatures in spite of nonmagnetic elements.¹⁴ This result strongly suggests the existence of intercluster electronic interaction between arrayed clusters. The K-density dependence of ferromagnetic properties has been interpreted in terms of the model of a weak ferromagnetism of itinerant electrons.^{43,44} In this model, it is assumed that narrow energy bands are realized by the intercluster electron transfer between $1s$ and $1p$ molecular orbitals of the K cluster. Ferromagnetism has been observed only under the condition that the Fermi energy is located at the $1p$ energy band. The electronic state, however, is not well understood yet. It is urgently necessary to elucidate the electronic state of arrayed K clusters in LTA from the viewpoint of optical properties.

In the present paper, the K-loading density is changed systematically in K-form LTA, and absorption and reflection spectra are analyzed. Three groups of absorp-

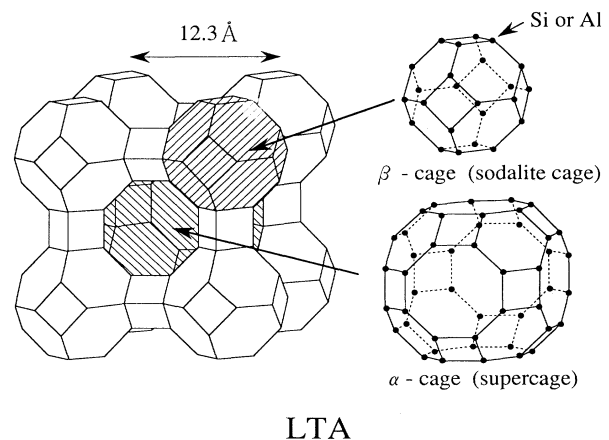


FIG. 1. Schematic representation of the framework structure of LTA. Oxygen atoms between Si and Al atoms are omitted. The α cages are connected by shared windows in a simple cubic structure.

tion or reflection bands appear between 0.5 and 3.5 eV depending on the K-loading density. The strongest band at ~ 2 eV is assigned to an SP-like state of K cluster. Other bands are basically interpreted in terms of the optical transition between narrow energy bands that originate from $1s$, $1p$, and $1d$ molecular orbitals of the K cluster. A Drude-like contribution is found in the analysis of reflection spectra.

II. EXPERIMENTAL PROCEDURES

A high-quality Na-form LTA powder was selected by means of both x-ray analysis and electron microscopy. Powder particles were cubic with the average size of $4 \mu\text{m}$, from a scanning electron micrograph. Na-form LTA powder was transformed into the K form by ion exchange in KCl aqueous solution, and the resulting powder was washed thoroughly with distilled water. The composition ratios were determined by atomic absorption spectrometry (AAS). The Si-to-Al, Na-to-Al, and K-to-Al ratios were 1.00, 0.08, and 0.83, respectively. The expected chemical formula is given as $\text{K}_{10}\text{NaHA}1_2\text{Si}_{12}\text{O}_{48}$. Slight hydrogenation was observed. This zeolite is abbreviated as K-LTA(1) hereafter.

The positions of K^+ ions in dehydrated K-LTA have been elucidated by x-ray structural analysis.^{45,46} Major K^+ ions are distributed around the center of a six-membered ring. Minor K^+ ion positions in K-LTA(1) used in the present experiment may, however, differ slightly from the results of above x-ray analysis, because the dehydration temperature is higher than theirs, as shown later. The positions of K^+ ions may change due to the K loading.

Original size K-LTA(1) and its ground powder were used for the present optical measurement. The ground powder was used only for the measurement of absorption spectra in the dilute K-loading region. Zeolite powder was dehydrated at 550°C for 15 h in a vacuum. The dehydration below 300°C (Refs. 45 and 46) was found to be insufficient, from the result of thermogravimetric analysis in vacuum, but that above 500°C is sufficient, as it scarcely showed a weight change due to the dehydration. The alkali-metal coloration was very sensitive to the degree of dehydration, because residual water molecules react with the loaded alkali metal. The dehydrated samples used in the present experiment scarcely showed such a reaction.

The dehydrated powder was sealed in a quartz tube together with a distilled K source and a small amount of helium gas. K was successively adsorbed into zeolite cage through the vapor phase by elevating the temperature to 160°C . Before the K loading, K-LTA(1) powder was white and did not exhibit any optical absorption between 0.4 and 6 eV. With increasing K density, the powder became dark blue, dark brick red, and finally russet gold at the saturation density. The K-loading density was proportional to the total adsorption time, except at the saturation density. The average number of guest K atoms was determined by means of AAS to be 7.3 per α cage at the saturation condition. The K-loading density of each sample was determined by both the reflection

spectrum analysis and the total adsorption time, and normalized by the AAS value.

Diffuse reflection spectroscopy was used for optical measurement. The measurement was performed at room temperature. The Kubelka-Munk function was used for the transformation of diffuse reflectivity into the absorption coefficient in dilutely loaded samples. The Kubelka-Munk function is given as $(1-r)^2/2r$, where r is the diffuse reflectivity. The sum of reflection R and transmission T of a powder particle is given by

$$R + T = \frac{4r}{(1+r)^2} \quad (1)$$

The derivation of this equation is given in the Appendix. Under the strong absorption condition $T \ll R$, the reflection spectrum is given by $4r/(1+r)^2$.

For comparison, we measured absorption spectra of Na-loaded Na-form FAU, K-loaded K-form FAU, and Rb-loaded Rb-form LTA. FAU with the Si-to-Al ratio of 2.8 was used. This zeolite is usually called Y, and is abbreviated FAU(2.8) hereafter. Rb-form LTA was obtained by the ion exchange of K-LTA(1) in RbCl aqueous solution. Alkali-metal-loaded zeolite powder was prepared according to a similar method.

III. EXPERIMENTAL RESULTS AND DISCUSSION

A. Absorption spectra of dilutely K-loaded K-LTA(1)

Absorption spectra of ground powder of K-loaded K-LTA(1) at room temperature are shown in Fig. 2. The K density increases in the order of curves 1–4. Dotted curves indicate the regions where the Kubelka-Munk function is no longer applicable due to the finite contribution from reflection of powder particles. The number

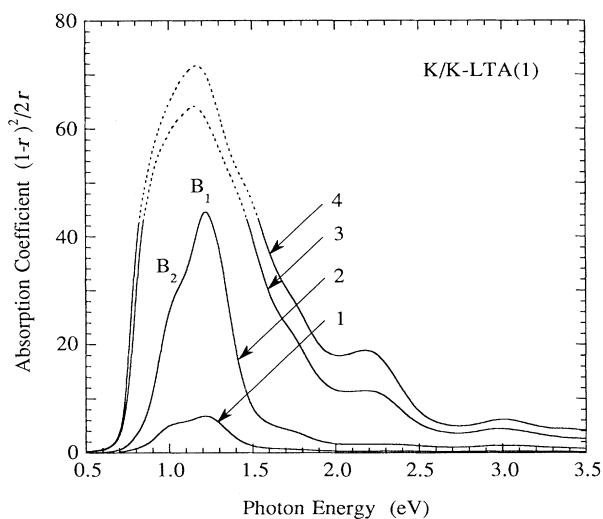


FIG. 2. Absorption spectra of dilutely K-loaded K-LTA(1) at room temperature. The K density increases in the order of curves 1–4. The dotted curve indicates the region where the diffuse reflectivity cannot be transformed correctly into the absorption coefficient using the Kubelka-Munk function.

density of guest K atoms is roughly estimated to be of the order of 0.1 per α cage in curve 2. Absorption bands appear at 1.0, 1.22, 1.75, 2.25, and 3.0 eV. The spectra are completely different from the atomic spectrum of K. The intensity of these bands increases with increasing K density. These bands originate from the same cluster, because the relative intensity is independent of K density. For convenience, strong bands at 1.22 and 1.0 eV are named B_1 and B_2 , respectively.

Here, we consider the potential of an electron in the space of zeolite. It is well understood that the covalent bonds are formed between framework atoms, while cations distributed in the space of the framework have no covalent bonds. The zeolite framework with Al content has a negative charge, while cations have a positive charge. Cations having no covalent bonds are drawn toward the rigid framework and repulsed by each other. The potential of an electron is due to repulsion and attraction to the framework and cations, respectively. If an electron is introduced there, the electron may be trapped by cations and repulsed by the framework. In this case, the intercation distance is important for the delocalization of electron wave function. If the outermost wave functions, the 4s orbital of the K atom, overlap each other, an electron may be delocalized in relevant cations. Hence, we can expect cations with a common delocalized electron in the α or β cages. This is a cationic cluster. The present K cluster is thought to have such structure.

In Na-form FAU, an Na_4^{3+} cluster has been generated in the β cage.³⁰⁻³⁴ In this cluster, an electron is confined by the attractive potential of 4 Na^+ ions, and is scarcely distributed at framework atoms. The absorption band has been observed at 500 nm (2.5 eV),³⁰ and is assigned to the transition between quantum levels (molecular orbitals) of the cluster. An equivalent K cluster, K_4^{3+} , is also observed in K-form FAU in ESR measurement.³² Figure 3 shows the absorption spectra of dilutely Na-adsorbed Na-FAU(2.8) and dilutely K-adsorbed K-FAU(2.8) at room temperature for comparison. Absorption bands of

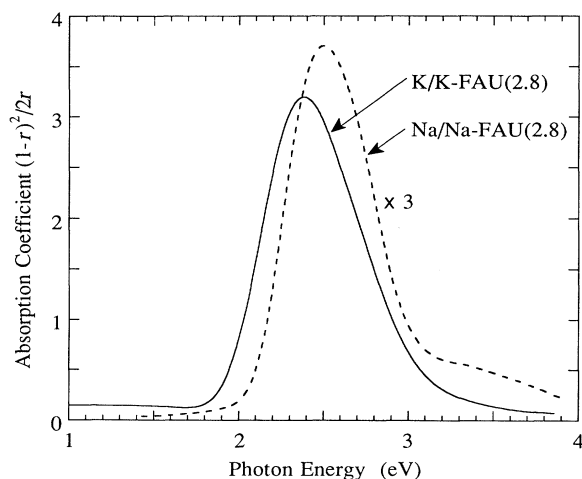


FIG. 3. Absorption spectra of dilutely K-loaded K-FAU(2.8) and dilutely Na-loaded Na-FAU(2.8) at room temperature.

Na_4^{3+} and K_4^{3+} clusters are observed at 2.5 and 2.4 eV, respectively. The existence of the Na_4^{3+} cluster of the present sample is confirmed by ESR measurement. The energy of absorption band has been quantitatively interpreted in terms of the model of 1s-1p transition of an electron trapped in a quantum sphere, with the inner diameter of the β cage, ~ 6.5 Å.

Main absorption bands B_1 and B_2 in Fig. 2 are redshifted considerably compared with that of K_4^{3+} in K-FAU(2.8). The redshift cannot be interpreted in terms of the optical transition model of an electron confined in the spherical potential with the inside diameter of the β cage. In LTA, however, there is another cage, the α cage. The 1s-1p transition energy is calculated to be 1.3 eV in the spherical potential with the inside diameter of the α cage, ~ 11 Å. The energies of bands B_1 and B_2 coincide well with this energy. Therefore, it is concluded from the optical measurement that these bands are due to the cluster in the α cage. Weak absorption bands at higher energies in Fig. 2 may be assigned to the transition from the 1s state to higher ones and/or to the charge-transfer excitation to an electronic state of the cluster in the β cage.

From the viewpoint of structural analysis, the following speculation is possible for K clusters in the α cage. There are many cations in the α cage of K-LTA. In dehydrated K-LTA, major K^+ ions are distributed in the α cage, 0.79 Å above the six-membered ring.⁴⁵ These cations are located at the corners of cube whose sides are 6.6 Å in length. This length is comparable with the lattice constant of K metal, 5.2 Å. According to the Herman-Skillman wave function,⁴⁷ the overlap integral between 4s orbitals of K atoms is 0.13 at the distance of 6.6 Å.⁴⁸ Therefore, if an electron is introduced there, a cationic cluster can be expected in the α cage including other cations of host and guest. A slight displacement of cation position may occur due to the electron-cation attractive interaction. This is one of the polaron effects. Some cations are also distributed near the window.⁴⁵ These cations may play an important role in the potential height between adjacent α cages, as discussed below.

The doublet structure of bands B_1 and B_2 , however, cannot be interpreted in terms of the model of the potential with the cubic symmetry of the α cage, because the energy of the 1p orbital degenerates in any cubic symmetry. The intercluster electron-transfer model is introduced in order to interpret the doublet structure of bands B_1 and B_2 . The wave function of the K cluster in the α cage is expected to overlap partly with those of adjacent clusters through windows, because of the decrease in the repulsive potential of the framework and of the cation distribution near the window. The ferromagnetic properties also strongly support the existence of the intercluster electron transfer.^{14,43,44} If the potential fluctuation due to the statistical distribution of K^+ ions can be neglected, electrons can travel resonantly and coherently in the periodic potential realized in the LTA framework. This indicates a narrow energy band for electrons. In this model, the optical transition basically reflects the joint density of state (JDOS) between two energy bands, if the wave-vector dependence of the transition probability can be neglected. A doublet structure can be expected in

JDOS of the $1s$ - $1p$ transition, because of the following energy dispersion of the $1p$ band. We consider a threefold degenerate energy band originating from $1p_x$, $1p_y$, and $1p_z$ molecular orbitals. The density of state of this band has a doublet structure, because the transfer energy of the $1p_x$ orbital for the x direction, for example, may be different from that for the y (or z) direction.

If the above interpretation is applicable to the electronic state of alkali-metal clusters in LTA, the absorption energy of the $1s$ - $1p$ transition may not depend largely on the kind of alkali metal, because the radial size of cluster potential in this model is basically determined not by that of cation potential but by that of the repulsive potential of the framework. In order to elucidate this point, the absorption spectrum is measured in dilutely Rb-loaded Rb-LTA(1) at room temperature, as shown in Fig. 4. The spectrum is quite similar to that in K shown in Fig. 2. This result suggests that the electronic state of Rb cluster is quite similar to that of K cluster. This result can be interpreted qualitatively as the nature of alkali-metal atoms, as follows. The empty-core radius of pseudopotential in alkali-metal atoms is significantly larger than that in other metal atoms,⁴⁹ and the ionization energy in alkali-metal atoms is much lower than that in other metal atoms. Hence, the position of cations may not be important to attain an effective potential for electrons, and the shape of potential may be determined mainly by the repulsive potential of framework.

In an actual system, the statistical distribution of K^+ ions may cause a potential fluctuation of electrons, because the potential will be deep at K^+ -rich cages. If the potential fluctuation is smaller than the transfer energy, the fluctuation effect can be taken into account in the band model consisting of both the localized electronic state due to the Anderson localization and the extended state, where the mobility edge is located between two states. In magnetic properties in K-loaded K-LTA(1), a disorder effect has been observed in the spin glass and the reentrant spin-glass phenomena.⁴⁴

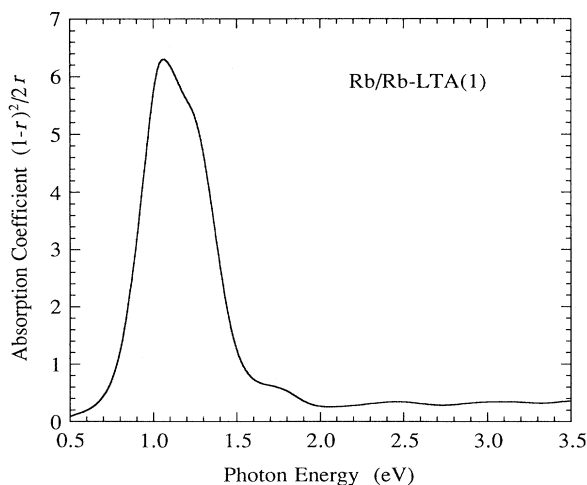


FIG. 4. Absorption spectrum of dilutely Rb-loaded Rb-LTA(1) at room temperature.

In Na clusters incorporated into Na-form LTA, the spectra are extremely different from those in K and Rb clusters. Na clusters are generated not only in the α cage but also in the β cage depending on the Na density. Clusters are inhomogeneously distributed due to the cohesion of Na.¹³ This is because the electron-cation (electron-phonon) interaction in Na is much stronger than that in K and Rb.

B. Reflection spectra of K-loaded K-LTA(1)

The reflection spectra are shown for K-loaded K-LTA(1) of original powder size by solid curves in Fig. 5. Dotted curves indicate the regions where the transmission T cannot be neglected. The K density increases in the order of curves 1–11. The average densities of guest K atoms per α cage are estimated to be 0.4, 0.8, 1.5, 2.4, 3.2, 4.1, 4.7, 5.4, 6.0, 6.6, and 7.3 in curves 1–11, respectively. Reflection bands appear and disappear depending on the K density.

Lower energy spectra are shown in the fine scale in Fig. 6 together with the absorption spectrum of curve 1 in Fig. 2. In curve 1, reflection structures due to bands B_1 and B_2 are discriminated. With increasing K density, they gradually disappear, and new bands with various marks appear at lower energies. Fine structures are seen around 0.7 eV. With K density approaching the saturation condition, these bands disappear.

If the interpretation is based on the energy-band model, the lower energy bands between 0.7 and 0.9 eV are assigned to the excitonic state of the $1s$ - $1p$ transition, as follows. An electron excitation from a filled band generally

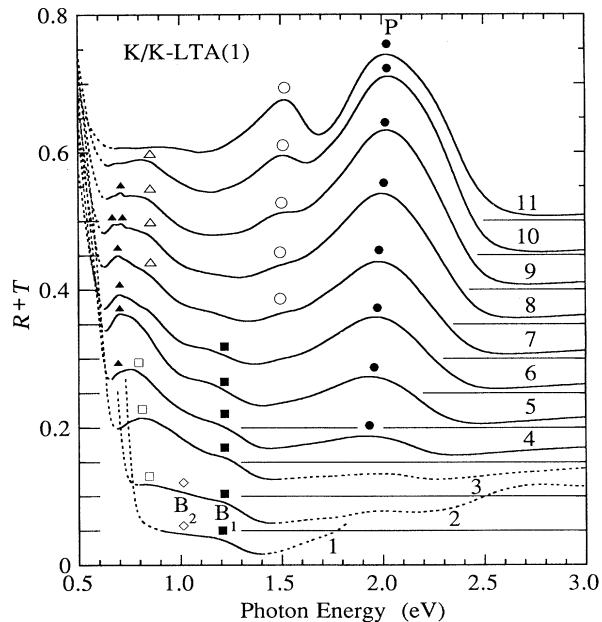


FIG. 5. K-density dependence of reflection spectra in K-loaded K-LTA(1) at room temperature (solid curves). The K density is saturated in curve 11. Broken curve indicates the region where the transmission cannot be neglected.

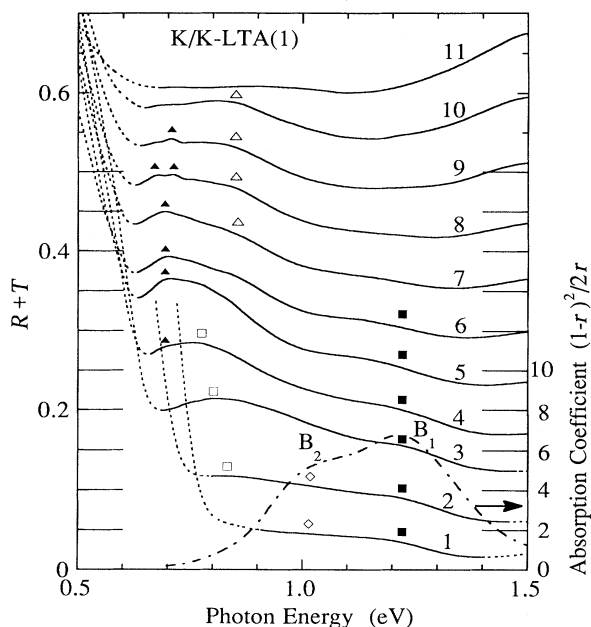


FIG. 6. Infrared parts of reflection spectra in K-loaded K-LTA(1) given in Fig. 5 and absorption spectrum given by curve 1 in Fig. 2. The dotted curves indicate the region where the transmission cannot be neglected.

leads to the generation of a hole. This hole will interact with the excited electron in the upper band. This electron-hole interaction can be neglected when it is screened by high density carriers. However, an excitonic effect can be expected in the case where the electron-hole interaction is not screened well. At intermediate K densities, the $1s$ band is completely filled with electrons, and a hole is generated there. The short-range attractive interaction between the $1s$ band hole and the $1p$ band excess electron may reduce the excitation energy, resulting in a prominent absorption band at the lower edge of the interband transition. Hence, the appearance of new bands at 0.7–0.9 eV is interpreted in terms of the electron-hole interaction model of $1s$ - $1p$ transition. The electron-hole interaction can be neglected in bands B_1 and B_2 in Fig. 2, because the $1s$ band is slightly filled with electrons and no electron-hole interaction occurs. The detailed origin of fine structures at 0.7 eV is not well known yet, but may be assigned to the excitonic states. The electron-hole interaction in metal has been observed in soft x-ray edge absorption of alkali metals^{50–53} and IR absorption of alkaline-earth metals.⁵³

Electron filling in the $1p$ energy band will lead to the disappearance of the $1s$ - $1p$ interband transition at the electron density of 8 per cluster, because of the Pauli exclusion principle. Hence, the weakness of bands around 0.8 eV at the highest K density in Figs. 5 and 6 is consistent with the $1s$ - $1p$ transition model.

The electron distribution in the $1p$ state leads to the occurrence of the optical transition from $1p$ to the upper electronic states. In the spherical potential with the inside diameter of the α cage of 11 Å, the $1d$ state is expect-

ed to be located 1.6 eV higher than the $1p$ state. In Fig. 5, the band at 1.5 eV appears and increases above the intermediate K density. The transition energy of 1.5 eV coincides well with the $1p$ - $1d$ energy. Hence, the reflection band at 1.5 eV can be interpreted in terms of the model of $1p$ - $1d$ interband transition.

Band P at ~ 2 eV appears at a relatively lower K density, and increases to become the largest band with increasing K density. Band P shows a slight blueshift with increasing K density. Band P has two components, as shown later. The oscillator strength of band P is much larger than unity per cluster at higher K densities, as shown later. This means that this band is due to the collective motion of electrons in a cluster. Therefore, band P is assigned to the SP-like excitation of the K cluster. Band P appears above an electron density of ~ 3 .

As observed in free alkali-metal clusters, the SP energy is rather insensitive to the cluster size or the number of atoms, but splits into several levels depending on the cluster shape.^{3,6} This result can be qualitatively understood to be an SP property as follows. The SP energy of a small metal particle is proportional to the square root of electron density in classical electromagnetic theory. The electron density of a free cluster is expected to be nearly constant due to the cohesion of constituent atoms. The cluster shape, however, changes with the symmetry of the electronic state. The SP energy can split into several levels when symmetry of the particle shape is degraded. Hence, the SP energy in free clusters is rather independent of the particle size but dependent on the shape. With increasing atomic size from Na to Cs, the electron density decreases. It is reasonable that the SP energy shifts to the lower-energy side in the increasing order of atomic size.¹⁰

For clusters incorporated into zeolite cages, however, the situation is different from that for free clusters. Electron density of the cluster may increase with increase of the average number of guest alkali-metal atoms, because the cluster size is expected to be fixed by the framework. However, the SP band in K-loaded K-LTA(1) does not show a marked blueshift with increasing K density. It seems that the SP energy is rather independent of the electron density of the cluster. The origin of this result is not well known yet, but the following qualitative interpretation is possible.

The theoretical calculation of cationic clusters reveals both a blueshift of SP energy and a significant exhaustion of the SP oscillator strength compared with those in neutral clusters.²⁴ Actually, the SP energy in Na_9^+ is higher than that in Na_8 .¹⁰ In anionic clusters, the theoretical calculation reveals a redshift of SP energy and a fragmentation of the oscillator strength compared with those of neutral clusters.²⁵ The above calculated results are closely related to the depth of effective potential for electrons. In LTA, clusters are highly cationic at lower K densities, because of the existence of many zeolite cations. In this case, excited-state electrons as well as ground-state electrons may be strongly confined in the α cage. If the space of LTA is filled with many K atoms, the height of confinement potential at windows may decrease. In this condition, excited electrons can be transferred to a great

extent into adjacent cages. As a result of a finite potential at the window, the SP energy may not increase in spite of the increase in electron density. From the above model, it can be reasonably stated that the oscillator strength of band *P* is saturated at higher *K* densities. The above model, however, is still quite speculative. Hence, further information is needed to determine the mechanism. As for ground-state electrons, an itinerancy of electrons is found as a Drude-like contribution in the analysis of the reflection spectra, as shown later.

In a strict sense, we cannot neglect the following problems in zeolite: (1) According to classical electromagnetic theory, dielectric polarization of the zeolite framework will contribute to the decrease in SP energy. (2) An excitation energy transfer between arrayed clusters may lead to a redshift in the transverse mode of the macroscopic polarization wave, namely the Frenkel exciton effect. This contribution is estimated to be less than 0.2 eV under the assumption of the Lorentz local field. (3) The potential symmetry is not spherical in the α cage of LTA. Hence, the SP state will split. The spectral shape of band *P* has a doublet structure ascribed to this effect, as stated later.

Finally, we perform curve fitting of the reflection spectra in the localized oscillator model in order to estimate the oscillator strength. The electron density can be easily estimated from the oscillator strength, because the total oscillator strength coincides with the total number of relevant electrons. The dielectric function $\epsilon(\omega)$ as a function of angular frequency ω is given by the equation

$$\epsilon(\omega) = \epsilon_0 + \frac{4\pi n e^2}{m} \sum_j \frac{f_j}{\omega_j^2 - \omega^2 - 2i\omega\gamma_j}, \quad (2)$$

where ϵ_0 is the frequency-independent term, n is the number density of oscillators, e is the charge of the electron, and f_j , ω_j , and γ_j are the oscillator strength, the resonant frequency, and the damping energy of the j th oscillator, respectively.

The polarization of the zeolite framework and cations

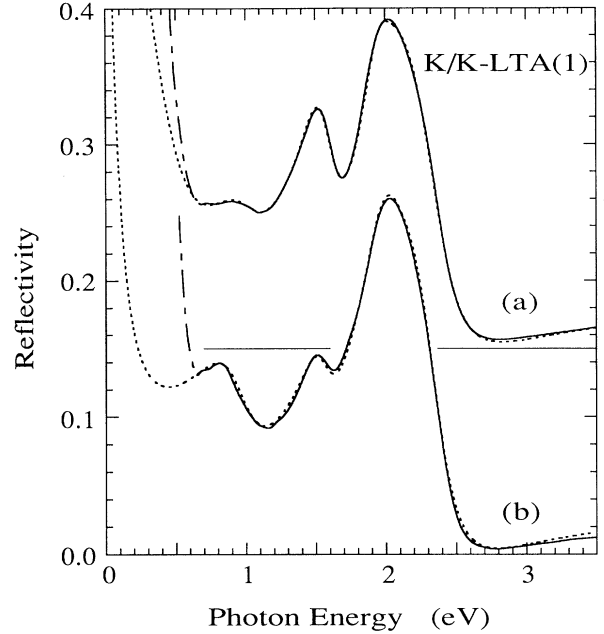


FIG. 7. Dotted curves in (a) and (b) indicate calculated reflection spectra fitted to the experimental spectra of curves 11 and 10 given in Fig. 5, respectively. Fitting parameters are given in Table I. Solid and chain curves indicate the experimental spectra.

is taken into account in ϵ_0 . The value of n is given by the number density of the α cage, $5.3 \times 10^{20} \text{ cm}^{-3}$. The calculated reflection spectra are indicated by the dotted curves in Figs. 7(a) and 7(b) which are fitted to experimental curves 11 and 10 in Fig. 5, respectively. The solid and chain curves indicate the experimental spectra. The fitting parameters are given in Table I. Band *P* corresponds to the 4th and 5th oscillators. The doublet components of the SP state are qualitatively interpreted in

TABLE I. Fitting parameters of reflection spectra in Figs. 7(a) and 7(b). Parameters ω_j , f_j , and γ_j are the energy, the oscillator strength, and the damping energy of the j th oscillator, respectively, and ϵ_0 is the frequency-independent part of dielectric function.

	j	ω_j (eV)	f_j	γ_j (eV)
Figure 7(a)				
$\epsilon_0 = 2.2$				
	1	0.0	1.9	0.75
	2	0.99	0.45	0.45
	3	1.53	1.46	0.27
	4	1.93	1.8	0.26
	5	2.06	2.1	0.47
Figure 7(b)				
$\epsilon_0 = 2.2$				
	1	0.0	0.8	1.0
	2	0.91	0.9	0.45
	3	1.53	0.75	0.26
	4	1.94	3.9	0.34
	5	2.14	0.6	0.38

terms of the dipole-dipole interaction theory of particles with O_h symmetry such as the α cage.⁵⁴ Such a doublet component has also been observed in Na clusters in Na-LTA(1).¹³ The total oscillator strengths of band P are 3.9 and 4.5 in curves a and b , respectively. These values correspond to the absorption cross sections of 4.3 and 4.9 \AA^2 , respectively. Both values are nearly the same as those obtained in free clusters.^{4,6}

For best fitting, we need to assume an oscillator at zero frequency. If we do not make this assumption, the fitting curve largely deviates from the experimental one. The oscillator at zero frequency indicates a Drude-like contribution from itinerant electrons realized in arrayed clusters. The magnetic properties have been interpreted in terms of itinerant electron ferromagnetism.^{43,44} Hence a finite electron density of states is expected at the Fermi surface. From the viewpoint of magnetic properties, the zero-frequency oscillator in the reflection spectrum is quite reasonable. The existence of itinerant electrons strongly suggests that the energy band model is basically applicable to the present system.

The total oscillator strengths are estimated to be 7.7 and 7.0 per α cage in curves a and b in Fig. 7, respectively. These values directly indicate the total number of 4s electrons per cluster. The value in saturated curve a , 7.7, coincides well with the AAS value of 7.3 atoms per unit cell. Hence, accurate curve fitting can be attained quantitatively.

IV. SUMMARY

K clusters are generated in the α cage of K-LTA(1) at the maximum K density of 7.3 atoms per cage. A reflection band with the largest oscillator strength is observed at ~ 2 eV, and assigned to the surface-plasmon-like state of the K cluster. Reflection or absorption bands between 0.8 and 1.2 eV are assigned to the $1s$ - $1p$ interband transition. The reflection band at 1.5 eV is assigned to the $1p$ - $1d$ interband transition. The Drude-like contribution from itinerant electrons is found in the analysis of reflection spectra.

ACKNOWLEDGMENTS

T.K. and Y.N. thank Professor Satoru Kunii for the ESR measurement. O.T. thanks Tosoh Corporation for support. This work was partly supported by a Research Grant from the Kurata Foundation and a Grant-in-Aid for Scientific Research from the Ministry of Education, Science and Culture of Japan.

APPENDIX: DERIVATION OF EQ. (1)

The diffuse reflection spectrum is known to be transformed into the absorption spectrum by the Kubelka-Munk function in the case of powder material with the isotropic and weak-absorption coefficient and a particle size greater than the wavelength of incident light. In order to reconsider the diffuse reflection process, we assume that the region $z < 0$ is filled with powder. An incident light passes into the powder in the $-z$ direction. Usually, the derivation of the Kubelka-Munk function

starts from the differential equations given by

$$-\frac{dP_1(z)}{dz} = -(K+S)P_1(z) + SP_2(z), \quad (\text{A1})$$

$$\frac{dP_2(z)}{dz} = -(K+S)P_2(z) + SP_1(z), \quad (\text{A2})$$

where $P_1(z)$ and $P_2(z)$ are the light energy flowing along the $-z$ and z directions, respectively, and $K/2$ and $S/2$ are the absorption coefficient and the scattering rate per unit length, respectively.

The diffuse reflection r is defined as

$$r = \frac{P_2(0)}{P_1(0)}. \quad (\text{A3})$$

We obtain the Kubelka-Munk function by solving Eqs. (A1) and (A2) as

$$\frac{K}{S} = \frac{(1-r)^2}{2r}. \quad (\text{A4})$$

Equations (A1) and (A2) are applicable when the transmitted light is sufficiently stronger than the light reflected by each powder particle, namely a weak-absorption limit. In the case of strong absorption (large K), however, the transmitted light intensity is no longer given by $1 - Kd/2$, where d is the size of powder particle.

Generally, the reflected light cannot be distinguished from the transmitted light in the diffuse reflection process, because both of them are included in the scattering process. The absorption coefficient K should be replaced by the product of the absorptive power A and S . The sum of reflection R and transmission T ($G = R + T$) is given by the subtraction of A , namely $G = 1 - A$. The direction of light energy becomes opposite at the rate of $GS/2$ in the diffuse reflection process. The remains of scattered light $GS/2$ are unchanged in the direction of light energy. Therefore, new versions of the equations are given as

$$-\frac{dP_1(z)}{dz} = -\left[A + \frac{G}{2}\right]SP_1(z) + \frac{G}{2}SP_2(z), \quad (\text{A5})$$

$$\frac{dP_2(z)}{dz} = -\left[A + \frac{G}{2}\right]SP_2(z) + \frac{G}{2}SP_1(z). \quad (\text{A6})$$

From the solution of the above equations at $z=0$, we obtain the equation

$$R + T = G = \frac{4r}{(1+r)^2}. \quad (\text{A7})$$

This equation is valid in any case of powder material with isotropic absorption coefficient and the particle size greater than the wavelength. In the limit of $r=1$, $R+T$ approaches unity.

In the weak-absorption limit, A is given by $1 - \exp(-Kd_{av}/2)$, where d_{av} is the average thickness of powder particles. Inserting the value of A into Eq. (A7),

we obtain the equation $\exp(-Kd_{av}/2) = 4r/(1+r)^2$. In the limit $Kd_{av} \ll 1$, Kd_{av} is given by $(1-r)^2/2r$. If d_{av} is assumed to be $d/2$, S is given by $1/d_{av}$. Finally, we obtain the relation

$$\frac{K}{S} = \frac{(1-r)^2}{2r}. \quad (\text{A8})$$

This is the Kubelka-Munk function.

- ¹K. Selby, M. Vollmer, J. Masui, V. Kresin, W. A. de Heer, and W. D. Knight, *Phys. Rev. B* **40**, 5417 (1989).
- ²K. Selby, V. Kresin, J. Masui, M. Vollmer, A. Scheidemann, and W. D. Knight, *Z. Phys. D* **19**, 43 (1991).
- ³K. Selby, V. Kresin, J. Masui, M. Vollmer, W. A. de Heer, A. Scheidemann, and W. D. Knight, *Phys. Rev. B* **43**, 4565 (1991).
- ⁴C. R. C. Wang, S. Pollack, D. Cameron, and M. M. Kappes, *J. Chem. Phys.* **93**, 3787 (1990).
- ⁵S. Pollack, C. R. C. Wang, and M. M. Kappes, *J. Chem. Phys.* **94**, 2496 (1991).
- ⁶C. R. C. Wang, S. Pollack, T. A. Dahlseid, G. M. Koretsky, and M. M. Kappes, *J. Chem. Phys.* **96**, 7931 (1992).
- ⁷H. Fallgren and T. P. Martin, *Chem. Phys. Lett.* **168**, 233 (1990).
- ⁸H. Fallgren, K. M. Brown, and T. P. Martin, *Z. Phys. D* **19**, 81 (1991).
- ⁹C. Brechignac, Ph. Cahuzac, F. Carlier, and J. Leygnier, *Chem. Phys. Lett.* **164**, 433 (1989).
- ¹⁰C. Brechignac, Ph. Cahuzac, F. Carlier, M. de Frutos, and J. Leygnier, *Z. Phys. D* **19**, 1 (1991).
- ¹¹C. Brechignac, Ph. Cahuzac, F. Carlier, M. de Frutos, and J. Leygnier, *Chem. Phys. Lett.* **189**, 28 (1992).
- ¹²C. Brechignac, Ph. Cahuzac, N. Kebaili, J. Leygnier, and A. Sarfati, *Phys. Rev. Lett.* **68**, 3916 (1992).
- ¹³T. Kodaira, Y. Nozue, and T. Goto, *Mol. Cryst. Liq. Cryst.* **218**, 55 (1992).
- ¹⁴Y. Nozue, T. Kodaira, and T. Goto, *Phys. Rev. Lett.* **68**, 3789 (1992).
- ¹⁵W. Eckardt, *Phys. Rev. B* **31**, 6360 (1985).
- ¹⁶Z. Penzar, W. Eckardt, and A. Rubio, *Phys. Rev. B* **42**, 5040 (1990).
- ¹⁷W. Eckardt, and Z. Penzar, *Phys. Rev. B* **43**, 1322 (1991).
- ¹⁸J. M. Pacheco, and W. Eckardt, *Phys. Rev. Lett.* **68**, 3964 (1992).
- ¹⁹S. Tomiya and K. Kawamura, *Z. Phys. D* **12**, 469 (1989).
- ²⁰C. Yannouleas, J. M. Pacheco, and R. A. Broglia, *Phys. Rev. B* **41**, 6088 (1990).
- ²¹C. Yannouleas and R. A. Broglia, *Europhys. Lett.* **15**, 843 (1991).
- ²²C. Yannouleas and R. A. Broglia, *Phys. Rev. A* **44**, 5793 (1991).
- ²³M. Bernath, C. Yannouleas, and R. A. Broglia, *Phys. Lett. A* **156**, 307 (1991).
- ²⁴C. Yannouleas, R. A. Broglia, M. Brack, and P. F. Bortignon, *Phys. Rev. Lett.* **63**, 255 (1989).
- ²⁵C. Yannouleas, *Chem. Phys. Lett.* **193**, 587 (1992).
- ²⁶V. Bonacic-Koutecky, M. M. Kappes, P. Fantucci, and J. Koutecky, *Chem. Phys. Lett.* **170**, 26 (1990).
- ²⁷S. Saito, S. B. Zhang, S. G. Louie, and M. L. Cohen, *Phys. Rev. B* **42**, 7391 (1990).
- ²⁸S. Saito, *Phys. Rev. B* **43**, 6804 (1991).
- ²⁹V. N. Bogomolov, *Usp. Fiz. Nauk* **124**, 171 (1978) [*Sov. Phys. Usp.* **21**, 77 (1978)].
- ³⁰P. H. Kasai, *J. Chem. Phys.* **43**, 3322 (1965).
- ³¹J. A. Rabo, C. L. Angell, P. H. Kasai, and V. Schomaker, *Disc. Faraday Soc.* **41**, 328 (1966).
- ³²M. R. Harrison, P. P. Edwards, J. Klinowski, and J. M. Thomas, *J. Solid State Chem.* **54**, 330 (1984).
- ³³P. P. Edwards, M. R. Harrison, J. Klinowski, S. Ramdas, J. M. Thomas, D. C. Johnson, and C. J. Page, *J. Chem. Soc. Chem. Commun.* **1984**, 982.
- ³⁴N. H. Heo and K. Seff, *J. Chem. Soc. Commun.* **1987**, 1225.
- ³⁵Y. Katayama, K. Maruyama, and H. Endo, *J. Non-Cryst. Solids* **117**, 485 (1990).
- ³⁶B. Xu, X. Chen, and L. Kevan, *J. Chem. Soc. Faraday Trans.* **87**, 3157 (1991).
- ³⁷K. W. Blazey, K. A. Müller, F. Blatter, and E. Schumacher, *Europhys. Lett.* **4**, 857 (1987).
- ³⁸F. Blatter, K. W. Blazey, and A. M. Portis, *Phys. Rev. B* **44**, 2800 (1991).
- ³⁹R. M. Barrer and J. F. Cole, *J. Phys. Chem. Solids* **29**, 1755 (1968).
- ⁴⁰K. Haug, V. Srdanov, G. Stucky, and H. Metiu, *J. Chem. Phys.* **96**, 3495 (1992).
- ⁴¹V. I. Srdanov, K. Haug, H. Metiu, and G. D. Stucky, *J. Phys. Chem.* **96**, 9039 (1992).
- ⁴²V. Gramlich and W. M. Meier, *Z. Kristallogr.* **133**, 134 (1971).
- ⁴³Y. Nozue, T. Kodaira, S. Ohwashi, and O. Terasaki, in *Proceedings of the 2nd Russian-Japan Meeting on Material Design Using Zeolite Space*, St. Petersburg, 1992, edited by V. P. Petranovskii and V. V. Poborchii (A. F. Ioffe Physical Technical Institute, St. Petersburg, Russia, 1992), p. 17.
- ⁴⁴Y. Nozue, T. Kodaira, S. Ohwashi, T. Goto, and O. Terasaki, *Phys. Rev. B* **48**, 12253 (1993).
- ⁴⁵P. C. W. Leung, D. B. Kunz, K. Seff, and I. E. Maxwell, *J. Phys. Chem.* **79**, 2157 (1975).
- ⁴⁶J. J. Pluth and J. V. Smith, *J. Phys. Chem.* **83**, 741 (1979).
- ⁴⁷F. Herman and S. Skillman, *Atomic Structure Calculations* (Prentice-Hall, Englewood Cliffs, NJ, 1963).
- ⁴⁸T. Kobayasi (private communication).
- ⁴⁹M. L. Cohen and V. Heine, in *Solid State Physics: Advances in Research and Applications*, edited by H. Ehrenreich, F. Seitz, and D. Turnbull (Academic, New York, 1970), Vol. 24.
- ⁵⁰G. D. Mahan, *Phys. Rev.* **163**, 612 (1967).
- ⁵¹C. Woodward and A. B. Kunz, *Phys. Rev. B* **39**, 7955 (1989).
- ⁵²T. Ishii, Y. Sakisaka, S. Yamaguchi, T. Hanyu, and H. Ishii, *J. Phys. Soc. Jpn.* **42**, 876 (1977).
- ⁵³D. J. Groh, A. B. Kunz, and C. R. Givens, *Phys. Rev. B* **41**, 8037 (1990).
- ⁵⁴R. Fuchs, *Phys. Rev. B* **11**, 1732 (1975).